



**HAL**  
open science

## Regional Variations of the Azores High Across Glacial-Interglacial Timescales

F Hevia-cruz, N D Sheldon, A. Hildenbrand, M T Hren, F O Marques, J.  
Carlut, F. Chabaux

► **To cite this version:**

F Hevia-cruz, N D Sheldon, A. Hildenbrand, M T Hren, F O Marques, et al.. Regional Variations of the Azores High Across Glacial-Interglacial Timescales. *Paleoceanography and Paleoclimatology*, 2024, 39 (5), pp.e2023PA004810. 10.1029/2023pa004810 . hal-04612708

**HAL Id: hal-04612708**

**<https://hal.science/hal-04612708>**

Submitted on 14 Jun 2024

**HAL** is a multi-disciplinary open access archive for the deposit and dissemination of scientific research documents, whether they are published or not. The documents may come from teaching and research institutions in France or abroad, or from public or private research centers.

L'archive ouverte pluridisciplinaire **HAL**, est destinée au dépôt et à la diffusion de documents scientifiques de niveau recherche, publiés ou non, émanant des établissements d'enseignement et de recherche français ou étrangers, des laboratoires publics ou privés.



Distributed under a Creative Commons Attribution - NonCommercial 4.0 International License

# Paleoceanography and Paleoclimatology



## RESEARCH ARTICLE

10.1029/2023PA004810

## Regional Variations of the Azores High Across Glacial-Interglacial Timescales

### Key Points:

- Precise K-Ar geochronology revealed pulses of soil formation over the past 1 Myr in the Azores, Central North Atlantic
- Paleosols' geochemistry recorded paleoclimatic conditions and revealed fast environmental changes
- Wet and warm climate resulted from persistent negative North Atlantic Oscillation conditions, favoring fast weathering of volcanic rocks

F. Hevia-Cruz<sup>1</sup> , N. D. Sheldon<sup>2</sup> , A. Hildenbrand<sup>1</sup>, M. T. Hren<sup>3</sup>, F. O. Marques<sup>4,7</sup> , J. Carlut<sup>5</sup> , and F. Chabaux<sup>6</sup>

<sup>1</sup>Université Paris-Saclay, CNRS UMR 8148, GEOPS, Orsay, France, <sup>2</sup>Department of Earth and Environmental Sciences, University of Michigan, Ann Arbor, Michigan, USA, <sup>3</sup>Department of Earth Sciences, University of Connecticut, Storrs, CT, USA, <sup>4</sup>Universidade de Lisboa, Lisboa, Portugal, <sup>5</sup>Université Paris Cité, CNRS UMR 7154, Institut de physique du globe de Paris, Paris, France, <sup>6</sup>Université de Strasbourg, CNRS UMR 7063, ITES (Institut Terre et Environnement de Strasbourg), Strasbourg, France, <sup>7</sup>Retired

### Supporting Information:

Supporting Information may be found in the online version of this article.

### Correspondence to:

F. Hevia-Cruz,  
francisco.hevia-cruz@universite-paris-saclay.fr

### Citation:

Hevia-Cruz, F., Sheldon, N. D., Hildenbrand, A., Hren, M. T., Marques, F. O., Carlut, J., & Chabaux, F. (2024). Regional variations of the Azores high across glacial-interglacial timescales. *Paleoceanography and Paleoclimatology*, 39, e2023PA004810. <https://doi.org/10.1029/2023PA004810>

Received 15 NOV 2023

Accepted 13 MAY 2024

### Author Contributions:

**Conceptualization:** F. Hevia-Cruz, N. D. Sheldon, A. Hildenbrand  
**Funding acquisition:** A. Hildenbrand  
**Investigation:** F. Hevia-Cruz, N. D. Sheldon, A. Hildenbrand, M. T. Hren, F. O. Marques, J. Carlut, F. Chabaux  
**Methodology:** F. Hevia-Cruz, N. D. Sheldon, A. Hildenbrand  
**Project administration:** A. Hildenbrand  
**Supervision:** A. Hildenbrand  
**Validation:** F. Hevia-Cruz, N. D. Sheldon, A. Hildenbrand  
**Visualization:** F. Hevia-Cruz

**Abstract** The late Quaternary paleoclimate of the North Atlantic region has been widely studied, but the local terrestrial response to broader climatic variations remains underexplored. The Azores Archipelago, influenced by the North Atlantic Oscillation (NAO) and the Azores High, is a strategic target to investigate such interactions. Here, paleosols developed in equilibrium with the atmosphere recorded environmental variations in their geochemistry, and volcanic units sealing those paleosols allow for their precise dating. Clay mineralogical transfer functions from paleosol geochemistry and geochronological data were used to track paleoclimatic and paleoecological changes in this region over the past 1.3 Myr. Mean annual precipitation and air temperature reconstructions range from 620 to 1,520 mm yr<sup>-1</sup> and 14–26°C, with the latter tightly coupled with previous reconstructions of sea surface temperature. New K-Ar ages evidence pulsed soil formation periods under weathering-favorable wet and warm conditions, suggesting periods of a persistent negative NAO with a weakened or more southern Azores High after glacial Terminations I, II, IV, V, IX, and X. Our humidity province reconstructions indicate a prevailing moist to wet forest under cool temperate to subtropical conditions, with less variability than continental Europe. A rapid paleoecological shift occurred at ~430 ka in São Miguel Island, probably associated with the high amplitude of Termination V. Paleoecological changes younger than 430 ka could be related to local, not large-scale, climate changes. Average past precipitations were ~170 mm yr<sup>-1</sup> lower than in the present, which suggests that modern weathering rates are higher than observed in our record.

**Plain Language Summary** In this work, we studied the local climate of the Azores volcanic islands in response to broader climatic changes over the past 1 million years. By studying the chemistry of paleosols—ancient soils incorporated into the geological record—we reconstructed the conditions of precipitation and temperature at the time of their formation. Air temperature reconstructions are similar to previous reconstructions of sea surface temperatures, suggesting a close relationship between atmospheric and sea surface temperatures in the North Atlantic region. The age determination of volcanic units allowed us to constrain the ages of paleosols. We observed that most paleosols developed quickly after the end of glacial periods, under wet and warm conditions that favored the fast transformation of volcanic products into soils. This indicates periods over which the Azores High—an atmospheric high-pressure system that impacts the Azores' climate—was weakened or centered farther to the south of its current position. The chemistry of the paleosols registered fast environmental changes and suggests that the present annual precipitations are higher than over the past million years, which could impact the local economic activities and even the global climate, due to the capture of atmospheric CO<sub>2</sub> through the weathering of volcanic rocks.

## 1. Introduction

The climate of the North Atlantic and neighboring regions is impacted by regional-scale oceanic and atmospheric currents. For instance, Kim et al. (2007) identified millennial-scale cooling trends off northwest Africa, associated with variations in the North Atlantic Subtropical Gyre and changes in the pressure gradient between the Icelandic Low and the Azores High (Figure 1a). The latter, also known as the North Atlantic Oscillation (NAO), has been the focus of several studies, due to its impact on the climate of densely populated areas, such as the east coast of North America and Western Europe (e.g., Wanner et al., 2001). Positive phases of the NAO bring humidity to

© 2024 The Authors.

This is an open access article under the terms of the [Creative Commons Attribution-NonCommercial License](https://creativecommons.org/licenses/by/4.0/), which permits use, distribution and reproduction in any medium, provided the original work is properly cited and is not used for commercial purposes.

**Writing – original draft:** F. Hevia-Cruz, N. D. Sheldon, A. Hildenbrand

**Writing – review & editing:** F. Hevia-Cruz, N. D. Sheldon, A. Hildenbrand, F. O. Marques, J. Carlut, F. Chabaux

Northern Europe, promote dryness in southern Europe, and track tropical cyclones closer to the East coast of the U.S., while negative phases of the NAO carry warmth and humidity to Southern Europe and Northern Africa (Cresswell-Clay et al., 2022, and references therein). The paleoclimate of the broader region has also been extensively studied for the late Quaternary, largely relying on the study of marine sediment cores. For example, Martrat et al. (2007) and Rodrigues et al. (2017) estimated the sea surface temperature (SST) over the late Quaternary in the central North Atlantic based on the study of phytoplanktonic alkenones, and Martin-Garcia (2019) tracked north-south migrations of the Arctic Front through the study of alkenone- and foraminifera-based SST reconstructions. Both studies consider the impacts of the NAO on the European climate. Nevertheless, the scarcity of terrestrial paleoclimatic archives makes it hard to compare the oceanic and terrestrial paleoclimates. Thatcher et al. (2020) tracked the teleconnection between the SST and the continental European climate during the Holocene through the study of  $\delta^{13}\text{C}$  and  $\delta^{18}\text{O}$  in stalagmites in Portugal. Nevertheless, stalagmites, as well as tree rings, are not often preserved deep enough in time to study the terrestrial impact of oceanic paleoclimatic changes at glacial-interglacial temporal scales. In summary, our current understanding of the relationship between oceanic and terrestrial climate remains limited for most of the Quaternary, particularly on volcanic islands, where terrestrial paleoclimatic archives are scarce. In this context, the Azores Archipelago represents a key target for studying the response of the local climate to broader drivers in the Central North Atlantic Ocean over the late Quaternary.

Directly under the influence of the Azores Current and the Azores High Pressure (Figure 1a; Cresswell-Clay et al., 2022; Frazão et al., 2022; Martin-Garcia, 2019), the Azores Archipelago encompasses nine volcanic islands spreading ~600 km over the triple junction of the North America, Nubia, and Eurasia lithospheric plates (Figure 1b), allowing observations and comparisons at local to regional scales. Most of these islands have been volcanically active over the past 1 million years (Myr), with periods of relative quiescence (e.g., Costa et al., 2014, 2015; Hildenbrand, Madureira, et al., 2008; Hildenbrand et al., 2012, 2014; Marques et al., 2018; Sibrant et al., 2015). This period is particularly interesting in terms of paleoclimate, as it is characterized by high-amplitude glacial-interglacial transitions (e.g., Lisiecki & Raymo, 2005; Martin-Garcia, 2019). In addition, the Azores Islands preserve numerous paleosols (PSs), ancient soils developed in contact with the atmosphere and incorporated into the geological record once sealed by volcanic deposits. Except when diagenesis is extensive, PSs record valuable environmental information including the paleoclimatic conditions under which they were formed (Sheldon & Tabor, 2009). Indeed, the geochemistry of both soils and PSs in non-anthropogenic systems results from the interaction of five factors: the parental rock, climate, topography, organic activity, and time (Jenny, 1941). Among these factors, the parental material composition and climate are dominant, as topography should not play a major role in the flat lowlands of volcanic islands, and organic activity depends on climate (White, 2005). Also, fast weathering occurs during the first few thousand years of soil formation, which tends to equilibrate due to cation depletion and the precipitation of stable clay minerals, limiting the impact of time, as indicated by several studies (Börker et al., 2019; Chadwick et al., 2022; Rad et al., 2011, 2013; Sowards et al., 2018). PSs developed on volcanic rocks have been extensively used to make paleoclimatic reconstructions in different volcanic contexts (e.g., de la Horra et al., 2012; Orr et al., 2021; Sheldon, 2006), including a recent study on São Miguel Island, at the eastern end of the Azores (Hevia-Cruz et al., 2024). They showed that PSs can effectively record fast climatic changes (glacial-interglacial transitions) during the volcanic lifespan of volcanic islands, with a good correlation with SSTs. The aim of this work is to understand the regional paleoclimatic evolution of the Azores Archipelago and to track variations of the Azores High-pressure system through a geochemical study of PSs in the islands of Pico, Faial and São Jorge (Central Azores, Figures 1b and 1c), combined with precise geochronological constraints.

## 2. Methods

### 2.1. Fieldwork Strategy

We carried out a fieldwork campaign in June 2022 to Pico, Faial and São Jorge islands, in the Central Azores (Figure 1). These islands were selected for several reasons: they are under the influence of the NAO (Figure 1a); the volcanic activity of these islands complements one another in time, providing a temporal window to study the climate of the past 1 Myr (Costa et al., 2014, 2015; Hildenbrand, Madureira, et al., 2008; Hildenbrand et al., 2012, 2014; Marques et al., 2018; Sibrant et al., 2015); and they preserve numerous PSs intercalated in their volcanic stratigraphy. In addition, the different islands of the Azores are distant enough from São Miguel Island to allow us to make regional comparisons with previous results (Hevia-Cruz et al., 2023, 2024), but close enough to each



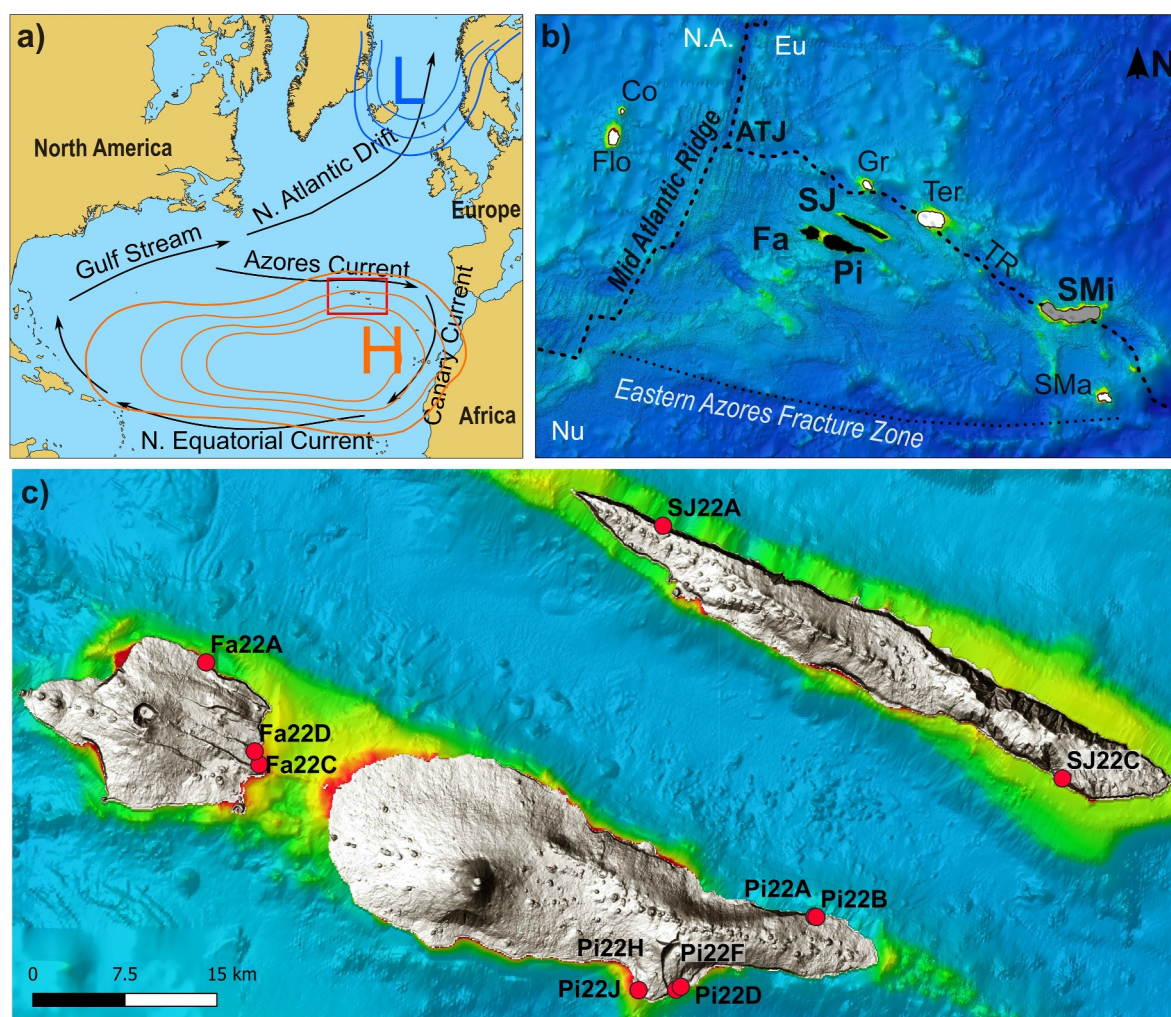


**Figure 1.** Location and general context of the Azores. (a) Scheme of the North Atlantic Subtropical Gyre (black arrows) and the atmospheric pressure systems: Azores High (orange “H”) and Icelandic Low (blue “L”); Cresswell-Clay et al., 2022; Frazão et al., 2022; Martin-Garcia, 2019). The red rectangle indicates the location of panel (b); (b) Distribution of the Azores islands and their tectonic context after Hildenbrand et al. (2014). In black are highlighted the Central Azores islands, studied in this work: Pico (Pi), Faial (Fa) and São Jorge (SJ). In gray is shown the previously studied São Miguel Island (SMi; Hevia-Cruz et al., 2024). In white are the islands not considered in this work: Flores (Flo), Corvo (Co), Graciosa (Gr), Terceira (Ter) and Santa Maria (SMa). ATJ: Triple junction of North America (N.A.), Nubia (Nu) and Eurasia (Eu) lithospheric plates. TR: Terceira Rift; (c) Location of the sampled paleosol profiles. Full stratigraphic profiles for each paleosol can be found in the Data Repository by Hevia-Cruz et al. (2023).

other to move between islands easily. We targeted PSs that were “bracketed” (under- and overlain) by volcanic units which enabled constraining their formation age and timing. We sampled 14 fresh lava flows for K-Ar geochronological analyses on groundmass separates. Our temporal constraint of PSs also includes six previously published ages (Costa et al., 2014, 2015; Hildenbrand et al., 2012). A total of 70 PS samples were collected over eleven PS profiles (Figure 1c), including parental rocks, for geochemical analyses. The superficial and the uppermost parts of the PSs were avoided or removed to prevent contamination with recently weathered or thermally altered materials, respectively.

## 2.2. K-Ar Geochronology

The unspiked K-Ar technique (Gillot & Cornette, 1986) has been extensively used to date lavas with low K content in the Azores Archipelago (e.g., Costa et al., 2014, 2015; Hevia-Cruz et al., 2024; Hildenbrand, Madureira, et al., 2008, 2012). The isolation of fresh groundmass through magnetic and heavy liquids separation ensures avoidance of inherited phenocrysts with excess Ar, obtaining eruption ages. K content and argon isotopes ( $^{40}\text{Ar}$  and  $^{36}\text{Ar}$ ) were measured separately in two aliquots of the same homogeneous preparation by flame

absorption and magnetic mass spectrometry, respectively. Standards were measured under the same conditions for quality control and calibration: MDO-G (Gillot et al., 1992) and BCR-2 (Wilson, 1997) for K; HD-B1 for  $^{40}\text{Ar}^*$ , with a recommended age of  $24.18 \pm 0.09$  Ma after Schwarz and Trieloff (2007). The decay constants and isotopic ratios employed are from Steiger and Jäger (1977) calculated after Renne et al. (1998). This technique allows for the measurement of precise ages, with a few thousand years as typical uncertainties. Further details about this method can be found in Gillot et al. (2006) and Hildenbrand et al. (2018).

### 2.3. Geochemistry

Those PS profiles with vertical continuity that were geochronologically constrainable were selected for geochemical analyses. Every horizon of each profile was sampled at least once, after removing  $\sim 10$  cm of the surface to avoid contamination, including the parental rock. After drying and powdering, the major elements of PS samples were analyzed in an iCap6500 ICP-OES (SARM, France; uncertainties generally  $<5\%$ , detailed in Table S1 in Supporting Information S1). Selected trace elements (REE, Zr, Rb) were analyzed in a Thermo-Scientific Element XR-HR-ICP-MS (GEOPS, France), and standards (BHVO-2, SL-1, BCR-2, BXN, JSd-1) were measured for quality assurance and control, with standard measurements within the recommended ranges ( $<10\%$ ; Hevia-Cruz et al., 2023). Major and trace elements were analyzed on all 70 samples.

Carbon and nitrogen concentrations were measured in a Costech ECS4010 analyzer (GRiTS lab, Earth and Environmental Sciences Department, University of Michigan; analytical precision better than 0.3 wt%), whereas  $\delta^{13}\text{C}$  measurements were made in a Costech ECS4010 elemental analyzer coupled to a MAT253 isotope-ratio mass spectrometer (University of Connecticut; analytical precision better than 0.1‰). C and N were measured on 41 samples, and  $\delta^{13}\text{C}$  on 35 samples.

### 2.4. Paleoclimatic and Floral Humidity Province Reconstructions

Major elements of B horizons were utilized to reconstruct mean annual precipitation (MAP) and mean annual air temperature (MAAT). B horizons are preferred for paleoclimatic reconstructions because their geochemistry results from equilibrium processes (e.g., accumulation of clays developed under atmospheric conditions by illuviation), and because they make it possible to avoid short-term (annual–multi-decadal) variability (Sheldon & Tabor, 2009; Tabor & Myers, 2015). The samples used for the paleoclimatic reconstructions correspond to B horizon samples with a Chemical Index of Alteration Minus Potash (CIA-K; Maynard, 1992) increase greater than 5 relative to the parent material; lower values were excluded based upon contamination or alteration after field and geochemical characterization of the whole profile. Two geochemical climofunctions based on the CIA-K and the Clayeyness Index (C; Retallack, 2001) were used as follows:

$\text{MAP} = 221.12e^{(0.0197 \times \text{CIA-K})}$ , where  $R^2 = 0.72$  and the standard error is  $\pm 181$  mm yr $^{-1}$  (Sheldon et al., 2002).

$\text{MAAT} = 46.9\text{C} + 4$ , where  $R^2 = 0.96$  and the total error is  $\pm 2^\circ\text{C}$  (Sheldon, 2006; Sheldon & Tabor, 2009).

These climofunctions were derived from modern soils all over the US and its territories, which encompass almost every climatic regime on Earth, except for tundra. By comparing the actual MAP and MAAT with the soils' geochemistry, Sheldon et al. (2002) and Sheldon (2006) found good correlations between climatic parameters and the geochemical composition of B horizons. The data set used for this corresponds to the US government soil survey by Marbut (1935). Both weathering indices were computed using molecular ratios (oxide wt% divided by molecular weight), with CIA-K calculated as  $100 \times \text{Al}_2\text{O}_3 / (\text{Al}_2\text{O}_3 + \text{CaO} + \text{Na}_2\text{O})$  and C as  $\text{Al}_2\text{O}_3 / \text{SiO}_2$ . In both cases, the uncertainties correspond to the standard error of the relation between the respective weathering index and the actual climatic parameters measured. All of the soils used for the climofunctions construction are younger than 100 ka (Sheldon, 2006; Sheldon et al., 2002), thus including the maximum formation time of all the PSs studied in the present work. Driese et al. (2005) performed a cross-validation of the MAP estimation using modern soils that were not part of the original data set used by Sheldon et al. (2002). They reconstructed the actual precipitation comfortably within error, and found consistency between MAP estimations and previous paleo-precipitation reconstructions in the Appalachian region based on independent proxies.

Humidity and floral provinces were reconstructed after Gulbranson et al. (2011), using their 33°N transect equations, as the temperatures of the Azores Archipelago are closer to that transect's temperature range. Energy from net primary production ( $E_{\text{NPP}}$ ) was calculated using their Equation 8; energy from precipitation ( $E_{\text{PPT}}$ ) with their Equation 7 and a value of  $26.2\% E_{\text{PPT}}$  (Inceptisol in their Table 2); evapotranspiration (ET) was calculated

with their Equation 6; and effective precipitation ( $P_{\text{eff}}$ ) with their Equation 11. All equations are included in Table S2. Reconstructions for São Miguel Island were based on the data reported by Hevia-Cruz et al. (2024).

### 3. Results

#### 3.1. Paleosols Characterization

PSs were classified as Andisols (those developed over Strombolian deposits) and Inceptisols (those developed over the upper brecciated parts of lava flows; Soil Survey Staff, 2014), or as Protosols according to the paleosol-specific classification of Mack et al. (1993). A horizons are often absent, and typical horizonation is Bw-C-R or Bt-C-R, similar to what was observed in São Miguel Island by Hevia-Cruz et al. (2024). PS profiles generally show a reddish coloration, with thicknesses between ~20 and ~100 cm, with an exception that reached ~5 m. Detailed physical descriptions (location, USDA soil taxonomy classification system, general profile and horizon descriptions, Munsell color, thicknesses and sampling depth) and temporal constraints of each PS and horizon can be found in Hevia-Cruz et al. (2023).

The 14 new K-Ar ages reported here range between  $1,326 \pm 21$  ka and  $46 \pm 2$  ka (Table 1). They are consistent with previously published ages and the general age distribution of Pico, Faial and São Jorge Islands (Costa et al., 2014, 2015; Hildenbrand, Madureira, et al., 2008, 2012, 2014; Marques et al., 2018; Sibrant et al., 2015; and references therein). Together with six previously published ages, the new data allow us to group PSs in clusters around ~1,325 ka, ~870–830 ka, ~325 ka, and ~110–45 ka (Figure 2).

The PSs were developed on micro-basaltic to basaltic Strombolian deposits and on basanitic to basaltic lava flows (Figure S1 in Supporting Information S1; Le Bas et al., 1986). The geochemistry and the texture of the parental rock are much more homogeneous in the Central Azores than what was observed in São Miguel Island, where differentiated (trachytic) tephra are more abundant (Hevia-Cruz et al., 2024). All profiles show an upward increase of CIA-K, except for profiles Pi22B and Pi22H2, both in Pico Island, for which CIA-K is steady (Pi22B) and decreases (Pi22H2) (Figure S2 in Supporting Information S1). The profiles generally show low variability of Ti/Al ratio (<20%, Figure S2 in Supporting Information S1), although some show an up-profile decrease in Ti/Al and some uppermost samples are very different compared to their parental rock (up to almost 60% difference, Figure S2 in Supporting Information S1). Carbon and nitrogen contents are low, all of them have <1.5% of carbon and <0.4% of nitrogen.  $\delta^{13}\text{C}$  ranges between  $-38.14\text{‰}$  and  $-11.32\text{‰}$ , with a mean of  $-25.84\text{‰}$ , mostly consistent with  $\text{C}_3$  vegetation (Tippel & Pagani, 2007). Full geochemical analyses are reported in Hevia-Cruz et al. (2023).

#### 3.2. Paleoclimatic Reconstructions

MAP and MAAT reconstructions are in the ranges  $\sim 620$ – $1,270$   $\text{mm yr}^{-1}$  and  $14$ – $26^\circ\text{C}$ , with one sample (FA22D2 in Table S3 in Supporting Information S1) that reaches  $\sim 1,520$   $\text{mm yr}^{-1}$  and almost  $28^\circ\text{C}$  (Figure 2; Table S3 in Supporting Information S1). The PSs Pi22B and Pi22H2 were not considered for paleoclimatic reconstructions, as their CIA-K do not increase up-profile, which might be associated with the incorporation of allochthonous material (such as ash-fall), and thus their geochemistry is not the result of equilibrium with the atmosphere (Figure S2 in Supporting Information S1; Sheldon & Tabor, 2009). The reconstructed MAPs are generally modestly lower than the present-day precipitation near sea level of  $\sim 1,100$   $\text{mm yr}^{-1}$  in Pico Island, and  $\sim 960$   $\text{mm yr}^{-1}$  in Faial Island (Figure 2; AEMET & IM, 2012). In turn, MAAT reconstructions are generally higher than, or similar to, the present mean temperatures of  $\sim 17.5^\circ\text{C}$  (Figure 2; AEMET & IM, 2012).

If we consider the entire time interval, the mean reconstructed MAPs and MAATs are slightly higher for the Central Azores compared to São Miguel (Figures 3a and 3d), consistent with present conditions (AEMET & IM, 2012). The only time interval with available data for both the Central Azores and São Miguel Island is for PSs younger than ~130 ka, that is, after Termination II. The MAP and MAAT reconstructions for this period overlap between the two areas, except for an exceptionally high MAAT of almost  $26^\circ\text{C}$  at ~114 ka in Faial Island, in the Central Azores (Figure 2b). Mean MAP and MAAT reconstructions (without full uncertainties) in São Miguel Island are generally lower than those of the Central Azores (Figures 3a–3f).

Regarding the  $\delta^{13}\text{C}$  of all the PSs (Figure 3g), besides being statistically equivalent, the mean value in the Central Azores is slightly lower (more negative) than in São Miguel. The same is observed for the PSs younger than 200



**Table 1**  
*K-Ar Ages Obtained in Groundmass Separates, Reported at 1σ Confidence Level*

| Name        | UTM N   | UTM E  | K%    | <sup>40</sup> Ar*% | <sup>40</sup> Ar* (10 <sup>10</sup> at/g) | Age [ka] | 1σ [ka] |
|-------------|---------|--------|-------|--------------------|---|----------|---------|
| Pi22D1      | 4249858 | 393884 | 1.064 | 2                  | 5.123                                     | 46       | 2       |
|             |         |        |       | 3                  | 5.037                                     | 45       | 2       |
|             |         |        |       | Mean               |   | 46       | 2       |
| (1) Pi10AE  | 4250217 | 394268 | -     | -                  | Mean                                      | 46       | 4       |
| Pi10Z       | 4255801 | 405466 | 0.893 | 2                  | 4.696                                     | 50       | 3       |
|             |         |        |       | 2                  | 4.140                                     | 44       | 3       |
|             |         |        |       | Mean               |   | 47       | 3       |
| Pi10Y       | 4255791 | 405337 | 0.975 | 1                  | 5.789                                     | 57       | 6       |
|             |         |        |       | 1                  | 5.455                                     | 54       | 6       |
|             |         |        |       | Mean               |   | 55       | 6       |
| Pi22G       | 4250101 | 394275 | 0.910 | 3                  | 5.927                                     | 62       | 3       |
|             |         |        |       | 3                  | 5.923                                     | 62       | 2       |
|             |         |        |       | Mean               |   | 62       | 2       |
| (1) Pi10L   | 4249872 | 393814 | -     | -                  | Mean                                      | 70       | 4       |
| Pi22E       | 4249824 | 393811 | 1.005 | 1                  | 7.092                                     | 68       | 7       |
|             |         |        |       | 1                  | 7.616                                     | 73       | 7       |
|             |         |        |       | Mean               |   | 70       | 7       |
| Pi22i       | 4249824 | 390836 | 1.011 | 3                  | 8.065                                     | 76       | 3       |
|             |         |        |       | 3                  | 7.893                                     | 75       | 3       |
|             |         |        |       | Mean               |   | 76       | 3       |
| Fa22B       | 4276511 | 355607 | 2.241 | 8                  | 24.126                                    | 103      | 2       |
|             |         |        |       | 9                  | 23.219                                    | 99       | 2       |
|             |         |        |       | Mean               |   | 101      | 2       |
| Pi22H       | 4249824 | 390836 | 1.280 | 5                  | 14.275                                    | 107      | 3       |
|             |         |        |       | 5                  | 14.003                                    | 105      | 3       |
|             |         |        |       | Mean               |   | 106      | 3       |
| (3) Fa10B   | 4276578 | 355673 | -     | -                  | Mean                                      | 127      | 3       |
| (2) Pi10H   | 4255843 | 405050 | -     | -                  | Mean                                      | 130      | 2       |
| SJ15A       | 4287585 | 392904 | 1.603 | 10                 | 52.977                                    | 316      | 6       |
|             |         |        |       | 8                  | 54.565                                    | 326      | 6       |
|             |         |        |       | 9                  | 52.766                                    | 315      | 6       |
|             |         |        |       | Mean <sup>a</sup>  |   | 319      | 3       |
| SJ22B       | 4287648 | 392831 | 1.740 | 10                 | 60.859                                    | 335      | 6       |
|             |         |        |       | 9                  | 59.157                                    | 325      | 6       |
|             |         |        |       | Mean               |   | 330      | 6       |
| Fa22E       | 4269211 | 359663 | 2.428 | 38                 | 211.007                                   | 832      | 12      |
|             |         |        |       | 36                 | 211.623                                   | 834      | 12      |
|             |         |        |       | Mean               |   | 833      | 12      |
| (3) AZ05-AL | 4268290 | 359795 | -     | -                  | Mean                                      | 846      | 12      |
| (3) AZ05-AM | 4268290 | 359795 | -     | -                  | Mean                                      | 848      | 12      |
| Fa22D       | 4269270 | 359553 | 1.429 | 27                 | 129.676                                   | 869      | 13      |
|             |         |        |       | 32                 | 129.145                                   | 865      | 13      |
|             |         |        |       | Mean               |   | 867      | 13      |
| SJ22D       | 4267068 | 425374 | 1.415 | 20                 | 193.106                                   | 1,306    | 20      |

**Table 1**  
*Continued*

| Name  | UTM N   | UTM E  | K%    | <sup>40</sup> Ar*% | <sup>40</sup> Ar* (10 <sup>10</sup> at/g) | Age [ka] | 1σ [ka] |
|-------|---------|--------|-------|--------------------|---|----------|---------|
|       |         |        |       | 19                 | 198.331                                   | 1,341    | 20      |
|       |         |        |       |                    | Mean                                      | 1,323    | 20      |
| SJ22C | 4267068 | 425374 | 1.372 | 17                 | 189.512                                   | 1,329    | 20      |
|       |         |        |       | 14                 | 188.706                                   | 1,323    | 21      |
|       |         |        |       |                    | Mean                                      | 1,326    | 21      |

*Note.* Decay constants and isotopic ratios from Steiger and Jäger (1977). Projection Zone 26S (WGS 84). <sup>a</sup>As the three individual ages of SJ15A are consistent, the mean age was weighted by the inverse of the variance. In italics are shown the ages previously reported by (1) Costa et al. (2014), (2) Costa et al. (2015), and (3) Hildenbrand et al. (2012). Detailed relations between lava flows and PS horizons can be found in Hevia-Cruz et al. (2023). Reported K% corresponds to mean values from at least two independent measurements with uncertainties lower than 1% (1σ).

ka (Figure 3h), but for those between 750 ka and 850 ka (Figure 3i) it is the opposite, although in this case, the δ<sup>13</sup>C values are even more similar than in the case of the younger PSs.

### 3.3. Paleoecological Reconstructions

Humidity province reconstructions oscillated mainly between moist and wet forests in both the Central Azores and São Miguel Island (full equations and calculations in Table S2). For the latter, the floral humidity province reconstruction (Figure 4a) evolved from a wet forest to a moist forest between ~820 and ~780 ka, then it passed quickly and for a short period to a wet forest at ~429 ka, to change back to a moist forest at ~427 ka. After ~170 ka, a wet forest prevailed, except at ~110 ka, when rainforest conditions were reached (Figure 4e). In the Central Azores, a moist forest prevailed between ~1,325 ka and ~847 ka. Then, between ~324 ka and ~95 ka a wet forest was developed, it passed to a moist forest at ~91 ka, and changed back to a wet forest from ~87 ka to ~58 ka (Figures 4c and 4e).

The Holdridge life zone classification system categorizes ecosystems based on temperature, precipitation, and potential evapotranspiration, visualized in a triangular diagram (Holdridge, 1947). It allows the visualization of dominant climate regimes, associated vegetation types, and potential responses to changing environmental conditions. According to this diagram, all PSs of São Miguel were formed under a moist forest in a humid province, ranging from cold to warm temperate latitudinal regions. The only exception occurs at ~430 ka, where it reached conditions between a warm temperate and a subtropical latitudinal region (Figure 4b). In the Central Azores, all PSs were developed in a moist forest in a humid province too, passing from a cool temperate latitudinal region at ~1,325 ka to subtropical at ~850 ka, to warm temperate at ~847 ka, and finally to a cool temperate region between ~324 and ~54 ka, except for 2 PSs developed in a warm temperate latitudinal region at ~114 and ~91 ka (Figure 4d).

At present, the vegetation cover of all the sampling sites corresponds to Coastal Woodland and Lowland Forests, with mean annual temperature and precipitations of ~14–20°C and ~1,000–1,600 mm yr<sup>-1</sup> (Elias et al., 2016). This corresponds to a Warm Temperate Moist Forest according to the same classifications used in Figure 4 after Gulbranson et al. (2011), which matches the younger PSs' humidity province (Figure 4d), although it is slightly wetter according to the Holdridge life zone classification (Figure 4c).

## 4. Discussion

### 4.1. Pulsed Soil Formation Tracked the Azores High's Position

As shown by our new geochronological constraints, the PSs studied in the Central Azores concentrate temporally after glacial stage terminations (Figure 2). This concentration of PSs after glacial terminations was also observed in the Eastern Azores (Hevia-Cruz et al., 2024), evidencing pulses of soil formation at a regional scale. A major sampling bias toward PSs formed after glaciation terminations is unlikely, as there were no PSs observed in the field in volcanic sections with ages attributable to glacial periods.



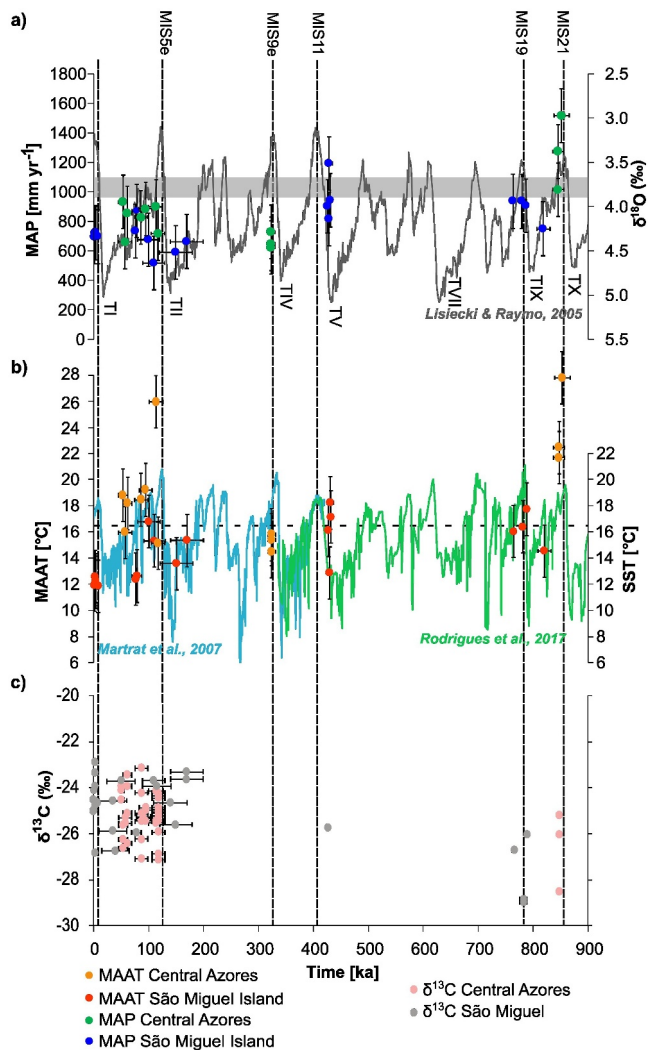


**Figure 2.** Mean annual precipitation and temperature reconstructions (MAP and MAAT, respectively) of the Central Azores, compared with data from São Miguel Island in the Eastern Azores after Hevia-Cruz et al. (2024). (a) MAP of the Azores. The gray line corresponds to the global  $\delta^{18}\text{O}$  of Lisiecki and Raymo (2005); (b) MAAT of the Azores. The blue and green lines correspond to Sea Surface Temperature (SST) in the North Atlantic Ocean after Martrat et al. (2007) and Rodrigues et al. (2017). (c)  $\delta^{13}\text{C}$  compilation from this work and Hevia-Cruz et al. (2024); high and low outlier values not shown. Vertical error bars are the standard deviation of the climofunctions (see 2.4), and the horizontal error bars are the maximum range of PS formation time (age difference between the volcanic units bracketing a PS). Graphically, the error bars of  $\delta^{13}\text{C}$  are included in the diameter of the circles. T letters with Roman numbers correspond to the termination of glaciations and MIS are Marine Isotope Stages. The horizontal gray area in (a) represents the present-day approximate MAP in coastal areas of the Azores, ranging from  $\sim 960 \text{ mm yr}^{-1}$  in Faial and  $\sim 980 \text{ mm yr}^{-1}$  in São Miguel to  $1,110 \text{ mm yr}^{-1}$  in Pico. The dashed horizontal line in (b) represents the coastal MAATs ( $17.5^\circ\text{C}$  in São Miguel,  $17.6^\circ\text{C}$  in Faial,  $17.4^\circ\text{C}$  in Pico; AEMET & IM, 2012; Hernandez et al., 2016).

According to Martin-Garcia (2019), the warmest and wettest interglacial stages in the North Atlantic and European regions occurred after extended ice-covered or prolonged glacial stages, such as Terminations IX and VIII, respectively. Our data show that PSs formed after those major glacial-interglacial transitions (Terminations I, II, IV, V, IX, and X in Figure 2b), all after maximal ice coverage glacial stages, presumably under particularly wet and warm conditions. This suggests that enhanced weathering promoted soil formation processes under relatively warm and wet conditions both in the Eastern and Central Azores. The only exception is Termination VII, for which no PSs were observed (Figure 2a). This could be due to a lack of outcrops, to inadequate conditions for soils to form (e.g., conditions that were too dry) or to the loss of soils to erosion, although we expect to find PSs over that time span in future field campaigns. It seems that, after Termination II, the PS production reached a maximum, with the highest number of PSs observed across the region. This might result from a particularly warm and wet interglacial stage, following a long and high ice volume glaciation as MIS6, consistent with the observations of Martin-Garcia (2019).

Those PSs formation periods could be revealing variations of the NAO and the position of the Azores High. Negative NAO allows the westerlies to have a southern position (Figure 5), carrying humidity closer to the Azores Archipelago and further into southern Europe (e.g., Hurrell & Van Loon, 1997; Pinto & Raible, 2012). For example, Hernandez et al. (2016) analyzed  $\sim 150$  years of precipitation in São Miguel Island, noting a good correlation between wetter years and negative NAO, with 82% of the days with heavy precipitation ( $>75 \text{ mm}$ ) coincident with negative NAO. Also, Amorim et al. (2017) observed that the lowest temperatures over the 2003–2013 period were coincident with positive NAO conditions. We propose that sustained negative NAO conditions could result in prolonged humid and warm periods in the Azores, thus favoring weathering and soil formation. This means that temporally close to Terminations I, II, IV, V, IX, and X, the Azores High was probably weakened or centered in a southern position (Figure 5b). Also, the higher humidity in the Central Azores compared to the eastern end of the archipelago could be related to its position 70–100 km to the north, closer to the Westerlies trajectories. This could be tested further if PSs are observed more to the north, as in Flores and Corvo islands, in the western end of the Azores archipelago (Figure 1b).

As observed by Cresswell-Clay et al. (2022), the present expansion of the Azores High might be unprecedented for the past 1,200 years, and furthermore, according to our observations, it could be unprecedented even for the past 1 Myr. However, the relatively sparse paleoclimatic data and especially the lack of information over glacial periods make it impossible to draw this conclusion definitively.

#### 4.2. Fast Paleoenvironmental Changes

Our MAP and MAAT reconstructions indicate fast paleoenvironmental changes, especially after Terminations X and V, and also after Termination II for MAAT. As well as what was observed in São Miguel Island, MAAT reconstructions in the Central Azores are consistent with previously published SSTs (Figures 2b and 6; Hevia-Cruz et al., 2024). This indicates the coupling of oceanic conditions to the atmosphere, as local air temperature seems to have been modulated by the SST, at least over the periods for which PSs could be dated.

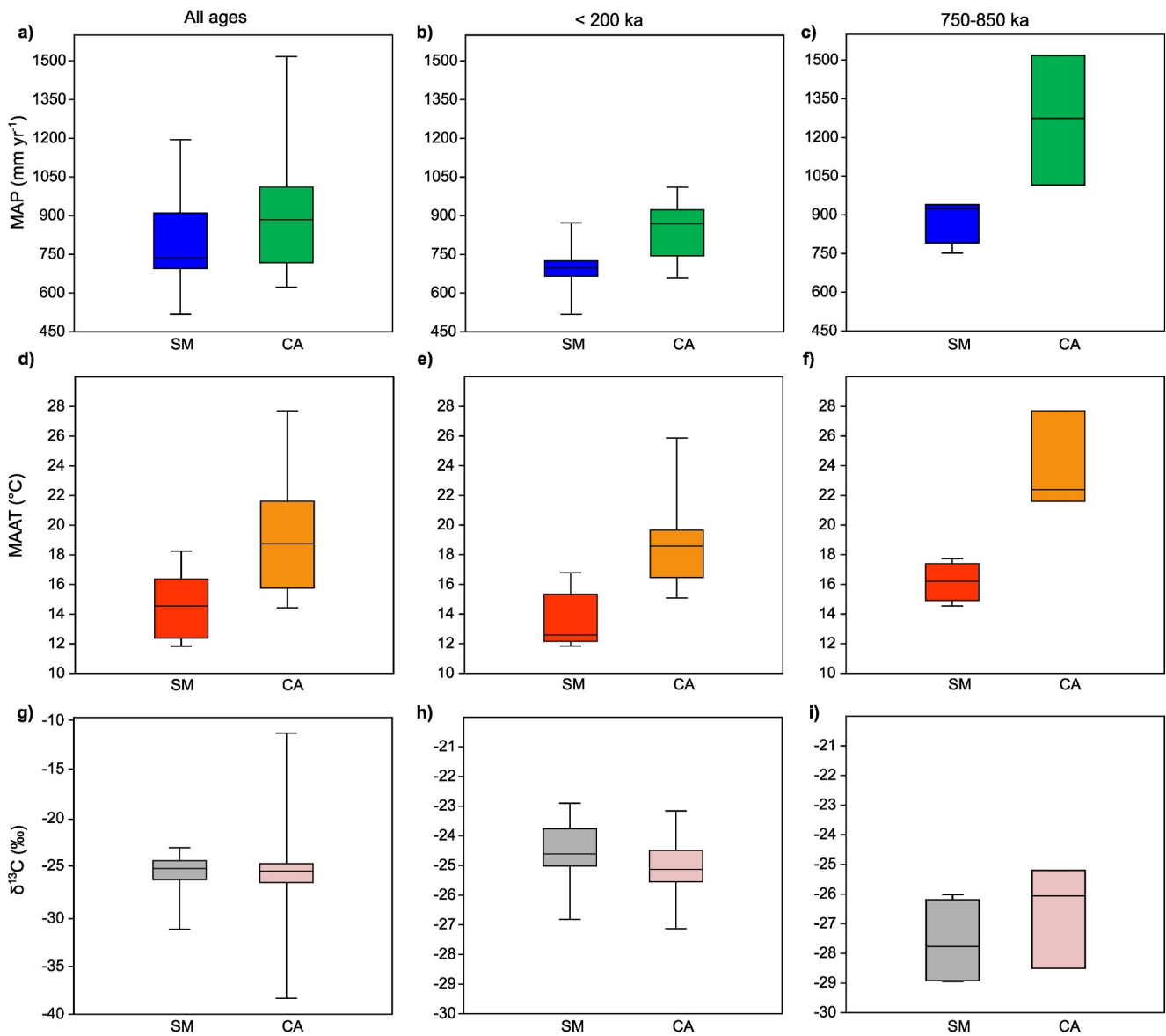


**Figure 3.** Box-and-whisker plot of MAP, MAAT,  $\delta^{13}\text{C}$  values of the Central Azores (CA) and São Miguel Island (SM). The left row includes all the studied paleosols (last  $\sim 1,325$  ka), the middle row those younger than 200 ka, and the right row those dated between 750 and 850 ka. São Miguel's data after Hevia-Cruz et al. (2024). The boxes go from quartile 1 to 3, the horizontal line of each box is the median, and the whiskers reach the minimum and maximum values.

Our  $\delta^{13}\text{C}$  values are consistent with  $\text{C}_3$  vegetation, consistent with the present-day low proportion of  $\text{C}_4$  plants in the Azores of only  $\sim 4\%$ , although almost half of its vegetation cover has been affected by human activity (Collins & Jones, 1986). The scarcity of water-stress thriving  $\text{C}_4$  vegetation could indicate the absence of long periods with prevailing dry conditions (e.g., Ghannoum, 2009; Taylor et al., 2011), also pointing to the south-centered or weakened Azores High. The  $\delta^{13}\text{C}$  values are consistent with our paleoecological reconstruction based on PS elemental geochemistry, which indicates that PSs were formed under a humid forest all over the last 1 Myr in the Eastern and Central Azores (Figure 4). This reasonably matches the present-day distribution of Coastal Woodlands and Lowland forests near the Azorean coasts (Elias et al., 2016). It also suggests that climate variations in the Azores were much less wide than in the Iberian Peninsula, where temperate arboreal and steppe vegetation replaced each other at the glacial-interglacial timescale (Margari et al., 2010; Sánchez-Goñi et al., 2008). Nevertheless, the lack of PSs formed during glacial stages makes it impossible to discard completely the idea of wider variations in the Azores, which could be further studied through the palynological study of marine sediment cores in the Azores region.

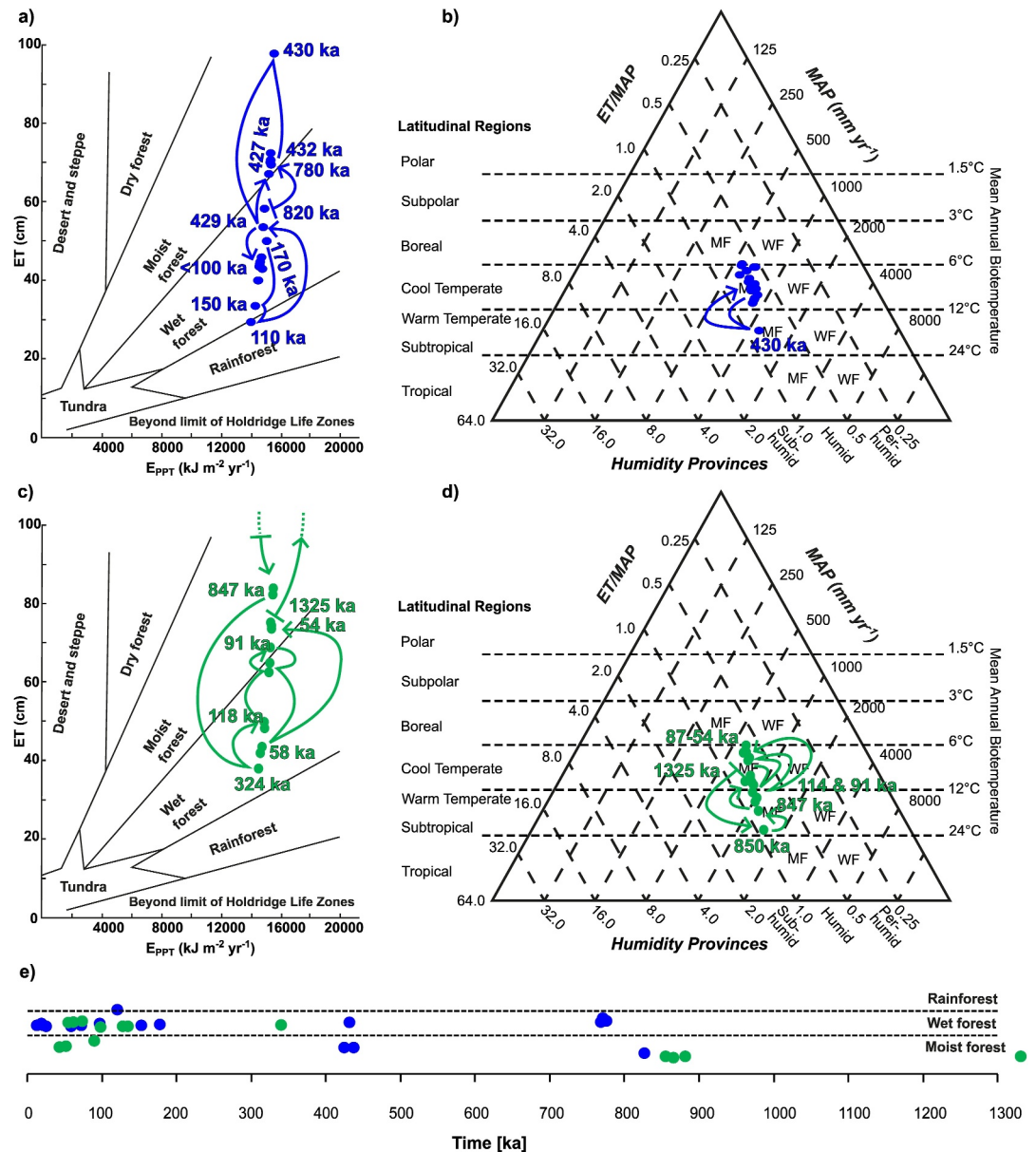


**Figure 4.** Paleosol-based floral humidity provinces and Holdridge life zones (Holdridge, 1947), modified after Gulbranson et al. (2011). In blue (a) and (b) are shown the ET,  $E_{PPT}$ , ET/MAP and MAP of São Miguel Island, after the data published by Hevia-Cruz et al. (2024), and in green (c) and (d) those of the Central Azores (full calculations in Table S2). The arrows show the temporal variations of the calculated values. (e) Shows the temporal variations of the paleosol-based floral humidity provinces with the same color code (São Miguel in blue and the Central Azores in green). MF: moist forest; WF: wet forest.

Although statistically equivalent, the slightly higher mean  $\delta^{13}C$  values of São Miguel Island for most PSs (Figures 3g and 3h) might suggest a higher proportion of  $C_4$  vegetation (e.g., Cerling et al., 1997; Tiplle & Pagani, 2007), indicating dryer conditions in the Eastern Azores. This slight  $\delta^{13}C$  difference is more evident for the PSs younger than 200 ka but still statistically equivalent. This is in agreement with our MAP reconstructions and with present-day conditions, which indicate higher MAP to the west. This reinforces the influence of the Azores High on the hydroclimate of the Azores. As discussed by Hevia-Cruz et al. (2024), this result does not seem to be impacted by the geochemistry of parental materials, as PSs were formed over short periods regardless of the parental rocks' geochemistry, both in São Miguel and in the Central Azores. The lack of PSs developed during similar periods in both the Central and Eastern Azores (except PSs younger than ~200 ka; Figure 2) prevents the possibility of making further regional comparisons, which could potentially be amended by carrying

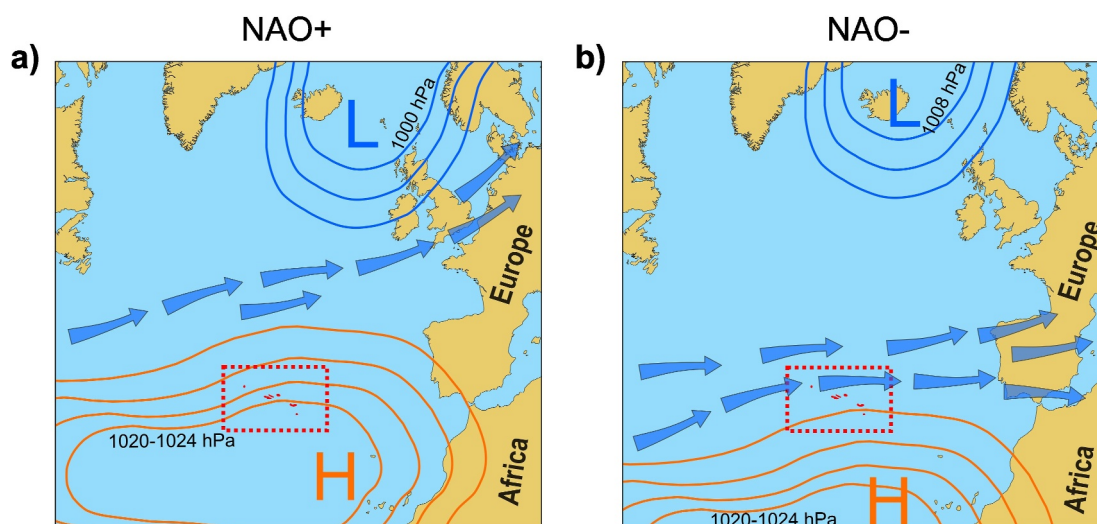


**Figure 5.** Current North Atlantic Oscillation pattern (NAO) and main Westerlies Winds trajectories (blue arrows) during (a) positive and (b) negative NAO extremes. The blue and orange lines represent isobar curves, centered in the Icelandic Low and the Azores High, respectively. Values of the Mean Sea Level Pressure from Cabos et al. (2020). The Azores Archipelago is highlighted in red, inside the red dashed rectangles.

out specific campaigns to try and fill the temporal gaps, including islands not yet investigated (Flores, Corvo, Terceira, Graciosa).

It was also possible to notice fast paleoenvironmental changes. Notably, we observed the change from a moist to a wet and back to a moist forest between  $\sim 430$  and  $\sim 427$  ka in São Miguel, which reached a maximum of ET at  $\sim 430$  ka, in response to high MAP and MAAT (Figures 2 and 4a, b). This could have resulted from a change from Coastal Woodlands to Lowland forests and back to Coastal Woodlands, the type of forest exclusively found near the coasts of the Azores today (Elias et al., 2016), and which are sensitive to moisture. Those two types of forests differ on their tree, shrub, herbaceous, epiphytic/epilithic and climbers species presence and proportions, with Coastal Woodlands dominated by *Erica azorica* and *Morella faya* and Lowland forests dominated by *Morella faya* and *Picconia azorica* (for details, see Table 3 of Elias et al., 2016). This period coincides with one of the glacial-interglacial transitions with higher amplitude over the past 1 Myr (from higher to lower  $\delta^{18}\text{O}$  compared to other transitions, as discussed in 4.1). In the Central Azores, a fast shift from wet to moist and back to a wet forest occurred between  $\sim 95$  and  $\sim 87$  ka (Figures 4c and 4e), and from wet to moist forest between  $\sim 58$  and  $\sim 54$  ka.

Nonetheless, those younger changes are not related to variations in global climatic conditions and might have been driven by local/regional changes in precipitation, such as variations in the NAO and the Azores High position.

Another temporal limitation is the range of applicability of our PS dating method. Profile SJ22C of São Jorge Island, dated at  $\sim 1,325 \pm 22$  ka, was not considered for comparison with São Miguel Island because it is substantially older than any PSs preserved there. The oldest PSs also have high absolute uncertainty (in kyr), which makes it difficult to assign a precise age to profile SJ22C.

### 4.3. Overestimated MAAT or High Air Temperature?

Our MAAT reconstructions are consistent with SST within uncertainties (in the range  $\sim 10$ – $19^\circ\text{C}$ ; Figures 2b and 6). Nevertheless, MAATs of two PSs of Faial Island greatly exceed previously reported SSTs: FA22D ( $\sim 850$  ka) by  $\sim 8^\circ\text{C}$  and FA22A ( $\sim 114$  ka) by  $\sim 5^\circ\text{C}$  (Figure 2b; Table S2). FA22A still has a reasonable temperature difference considering uncertainties according to Hren and Sheldon (2012), who contrasted the temperatures between the air and the surface of water bodies. Using their Equation 2, we obtain differences of  $\sim 6^\circ\text{C}$  between MAAT and SST, which can explain the difference of

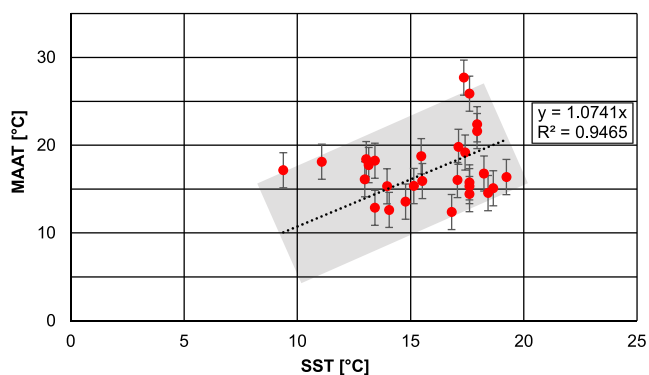


**Figure 6.** Linear correlation between mean annual air temperature reconstructions based on the paleosols geochemistry (MAAT) and Sea Surface Temperatures (SST) after Martrat et al. (2007) and Rodrigues et al. (2017). The vertical error bars correspond to the MAAT standard deviation after Sheldon (2006), and the gray area corresponds to the maximum difference between MAAT and SST according to Hren and Sheldon (2012).



FA22A, but not that of FA22D. This suggests that the MAAT of FA22D might have been overestimated. This can be attributed to the parental rock of FA22D, an alkaline basalt particularly rich (~50%) in feldspars up to 1 cm in diameter, which are very easy to weather compared to other minerals (e.g., Brantley et al., 2023, and references therein), resulting in amplified Clayeyness (Al/Si) and overestimated MAAT reconstructions. Nevertheless, the parental rock of FA22A is a fresh aphyric basalt, and there is no reason to think that it could be affected by its parental rock. Instead, it could be indicating particularly high atmospheric temperatures compared to SST. Further studies focusing on those two periods could elucidate this matter. This highlights the importance of the parental rock texture and composition in the rate of weathering processes, as observed in previous works (e.g., Berner & Kothavala, 2001; Chesworth, 1973; Hevia-Cruz et al., 2024; Sheldon, 2003; West et al., 2005).

#### 4.4. Broader Implications

As current precipitations and temperatures are higher than most of our MAP and MAAT reconstructions in this archipelago (Figure 2; AEMET & IM, 2012), it is probable that weathering is enhanced in the present, and may further increase in the near future due to accelerated anthropogenic climate change. Indeed, the Azores are expected to have an increase in mean annual air temperatures with no major variations in annual precipitation, although climatic models forecast wetter winters and drier conditions from spring to autumn (e.g., Meirrelles et al., 2022; Santos et al., 2004). This could have further implications for the stability of these volcanic islands, as intense precipitation can enhance riverine erosion (Hildenbrand, Gillot, & Marlin, 2008) and trigger landslides due to the hydration of clay-rich horizons such as PSs (Bolla et al., 2020).

Present enhanced weathering is consistent with the observations of Louvat and Allègre (1998), who estimated high chemical and mechanical erosion rates from the chemistry of rivers in the eastern part of São Miguel Island. This has important consequences for local human activities, which are highly based on agriculture and cattle raising, for example, by changing soil fertility and productivity (Melo et al., 2022). At a broader scale, the weathering of volcanic rocks, especially of volcanic islands, plays a major role in the global CO<sub>2</sub> cycle (e.g., Dessert et al., 2003; Gaillardet et al., 1999). Climate variations on this island affect weathering rates, which in turn, globally, can affect atmospheric CO<sub>2</sub>.

### 5. Conclusions

Paleosol geochemistry recorded fast paleoclimatic and paleoecological changes over the Central Azores (e.g., ~3 kyr after Termination V), and revealed periods of enhanced weathering, as previously observed in another island in the Eastern Azores (Hevia-Cruz et al., 2024). These relatively warm and wet periods were probably a consequence of a persistent negative North Atlantic Oscillation condition, with a weakened or south-centered Azores High. Despite some temporal and sampling limitations, as a result of a discontinuous development of paleosols and variable volcanic activity through time, paleosols represent a great proxy to study the paleoclimate to better understand the local, terrestrial response to global climatic forcing. Further studies in other islands of this archipelago could help improve our paleoclimatic reconstructions and our understanding of the teleconnection between marine and terrestrial climate.

According to our data, the Azores are experiencing wetter conditions than over most of the time slices of the past 1 Myr for which we could reconstruct mean annual precipitations. This potentially has local impacts on human activities, but also at broader scales, as the weathering of volcanic islands plays a major role in the global carbon cycle. Further studies in other islands of the archipelago, complemented with analyses in stream waters and marine sediments, could help elucidate the full impact of ongoing climate change on the weathering of volcanic islands.

#### Conflict of Interest

The authors declare no conflicts of interest relevant to this study.

#### Data Availability Statement

The detailed paleosol descriptions, and the geochemical and geochronological data of this study, including those used for paleoenvironmental reconstructions, are available at Mendeley Data repository by Hevia-Cruz et al. (2023) with CC BY 4.0.

## Acknowledgments

This work was supported by the CNRS-INSU TelluS-SYSTER program 2022–2023. FH-C. acknowledges the French MESRI doctoral program (2020–2023) and the Graduate School Géosciences Climat Environnement Planètes. NDS was supported by a visiting professor fellowship to Université Paris-Saclay. We thank Gaël Monvoisin and Frédéric Haurine for their help with sample leaching and geochemical analyses, and Valerie Godard for thin section preparation. This is LGMT contribution number 190.

## References

- AEMET & IMInstituto de Meteorología Portugal. (2012). Atlas Climático de los Archipiélagos de Canarias, Madeira y Azores. *Agencia Estatal de Meteorología de España e Instituto de Meteorología de Portugal*. <https://doi.org/10.31978/281-12-006-X>
- Amorim, P., Peran, A. D., Pham, C. K., Juliano, M., Cardigos, F., Tempera, F., & Morato, T. (2017). Overview of the ocean climatology and its variability in the Azores region of the North Atlantic including environmental characteristics at the seabed. *Frontiers in Marine Science*, *4*, 56. <https://doi.org/10.3389/fmars.2017.00056>
- Berner, R. A., & Kothavala, Z. (2001). GEOCARB III: A revised model of atmospheric CO<sub>2</sub> over Phanerozoic time. *American Journal of Science*, *301*(2), 182–204. <https://doi.org/10.2475/ajs.301.2.182>
- Bolla, A., Paronuzzi, P., Pinto, D., Lenaz, D., & Del Fabbro, M. (2020). Mineralogical and geotechnical characterization of the clay layers within the basal shear zone of the 1963 Vajont landslide. *Geosciences*, *10*(9), 360. <https://doi.org/10.3390/geosciences10090360>
- Börker, J., Hartmann, J., Romero-Mujalli, G., & Li, G. (2019). Aging of basalt volcanic systems and decreasing CO<sub>2</sub> consumption by weathering. *Earth Surface Dynamics*, *7*(1), 191–197. <https://doi.org/10.5194/esurf-7-191-2019>
- Brantley, S. L., Shaughnessy, A., Lebedeva, M. I., & Balashov, V. N. (2023). How temperature-dependent silicate weathering acts as Earth's geological thermostat. *Science*, *379*(6630), 382–389. <https://doi.org/10.1126/science.add2922>
- Cabos, W., de la Vara, A., Álvarez-García, F. J., Sánchez, E., Sieck, K., Pérez-Sanz, J. I., et al. (2020). Impact of ocean-atmosphere coupling on regional climate: The Iberian Peninsula case. *Climate Dynamics*, *54*(9–10), 4441–4467. <https://doi.org/10.1007/s00382-020-05238-x>
- Cerling, T. E., Harris, J. M., MacFadden, B. J., Leakey, M. G., Quade, J., Eisenmann, V., & Ehleringer, J. R. (1997). Global vegetation change through the Miocene/Pliocene boundary. *Nature*, *389*(6647), 153–158. <https://doi.org/10.1038/38229>
- Chadwick, O. A., Chorover, J., Chadwick, K. D., Bateman, J. B., Slessarev, E. W., Kramer, M., et al. (2022). Constraints of climate and age on soil development in Hawai'i. In *Biogeochemistry of the critical zone* (pp. 49–88). Springer International Publishing. [https://doi.org/10.1007/978-3-030-95921-0\\_3](https://doi.org/10.1007/978-3-030-95921-0_3)
- Chesworth, W. (1973). The parent rock effect in the genesis of soil. *Geoderma*, *10*(3), 215–225. [https://doi.org/10.1016/0016-7061\(73\)90064-5](https://doi.org/10.1016/0016-7061(73)90064-5)
- Collins, R. P., & Jones, M. B. (1986). The influence of climatic factors on the distribution of C4 plant in Europe. *Vegetation*, *64*(2–3), 121–129. <https://doi.org/10.1007/BF00044788>
- Costa, A. C. G., Hildenbrand, A., Marques, F. O., Sibrant, A. L. R., & de Campos, A. S. (2015). Catastrophic flank collapses and slumping in Pico Island during the last 130 kyr (Pico-Faial ridge, Azores Triple Junction). *Journal of Volcanology and Geothermal Research*, *302*, 33–46. <https://doi.org/10.1016/j.jvolgeores.2015.06.008>
- Costa, A. C. G., Marques, F. O., Hildenbrand, A., Sibrant, A. L. R., & Catita, C. M. S. (2014). Large-scale catastrophic flank collapses in a steep volcanic ridge: The Pico-Faial ridge, Azores triple junction. *Journal of Volcanology and Geothermal Research*, *272*, 111–125. <https://doi.org/10.1016/j.jvolgeores.2014.01.002>
- Cresswell-Clay, N., Ummenhofer, C. C., Thatcher, D. L., Wanamaker, A. D., Denniston, R. F., Asmerom, Y., & Polyak, V. J. (2022). Twentieth-century Azores high expansion unprecedented in the past 1,200 years. *Nature Geoscience*, *15*(7), 548–553. <https://doi.org/10.1038/s41561-022-00971-w>
- De la Horra, R., Galán-Abellán, A. B., López-Gómez, J., Sheldon, N. D., Barrenechea, J. F., Luque, F. J., et al. (2012). Paleoenvironmental changes during the continental Middle–Late Permian transition at the SE Iberian Ranges, Spain. *Global and Planetary Change*, *94*, 46–61. <https://doi.org/10.1016/j.gloplacha.2012.06.008>
- Dessert, C., Dupré, B., Gaillardet, J., François, L. M., & Allègre, C. J. (2003). Basalt weathering laws and the impact of basalt weathering on the global carbon cycle. *Chemical Geology*, *202*(3–4), 257–273. <https://doi.org/10.1016/j.chemgeo.2002.10.001>
- Driese, S. G., Nordt, L. C., Lynn, W. C., Stiles, C. A., Mora, C. I., & Wilding, L. P. (2005). Distinguishing climate in the soil record using chemical trends in a Vertisol climosequence from the Texas Coast Prairie, and application to interpreting Paleozoic paleosols in the Appalachian Basin, USA. *Journal of Sedimentary Research*, *75*(3), 339–349. <https://doi.org/10.2110/jsr.2005.027>
- Elias, R. B., Gil, A., Silva, L., Fernández-Palacios, J. M., Azevedo, E. B., & Reis, F. (2016). Natural zonal vegetation of the Azores Islands: Characterization and potential distribution. *Phytocoenologia*, *46*(2), 107–123. <https://doi.org/10.1127/phyto/2016/0132>
- Frazão, H. C., Prien, R. D., Schulz-Bull, D. E., Seidov, D., & Waniak, J. J. (2022). The forgotten Azores current: A long-term perspective. *Frontiers in Marine Science*, *9*, 842251. <https://doi.org/10.3389/fmars.2022.842251>
- Gaillardet, J., Dupré, B., Louvat, P., & Allegre, C. J. (1999). Global silicate weathering and CO<sub>2</sub> consumption rates deduced from the chemistry of large rivers. *Chemical Geology*, *159*(1–4), 3–30. [https://doi.org/10.1016/S0009-2541\(99\)00031-5](https://doi.org/10.1016/S0009-2541(99)00031-5)
- Ghannoum, O. (2009). C4 photosynthesis and water stress. *Annals of Botany*, *103*(4), 635–644. <https://doi.org/10.1093/aob/mcn093>
- Gillot, P., Albore-Livadie, C., Lefèvre, J., & Hildebrand, A. (2006). The K/Ar dating method: Principle, analytical techniques, and application to Holocene volcanic eruptions in southern Italy. *The K/Ar Dating Method*, 1000–1011.
- Gillot, P., & Comette, Y. (1986). The Cassinole technique for potassium—Argon dating, precision and accuracy: Examples from the Late Pleistocene to recent volcanics from southern Italy. *Chemical Geology: Isotope Geoscience section*, *59*, 205–222. [https://doi.org/10.1016/0168-9622\(86\)90072-2](https://doi.org/10.1016/0168-9622(86)90072-2)
- Gillot, P. Y., Cornette, Y., Max, N., & Floris, B. (1992). Two reference materials, trachytes MDO-G and ISH-G, for argon dating (K-Ar and 40Ar/39Ar) of Pleistocene and Holocene rocks. *Geostandards Newsletter*, *16*(1), 55–60. <https://doi.org/10.1111/j.1751-908X.1992.tb00487.x>
- Gulbranson, E. L., Montanez, I. P., & Tabor, N. J. (2011). A proxy for humidity and floral province from paleosols. *The Journal of Geology*, *119*(6), 559–573. <https://doi.org/10.1086/661975>
- Hernández, A., Kutiel, H., Trigo, R., Valente, M., Sigró, J., Cropper, T., & Santo, E. (2016). New Azores archipelago daily precipitation dataset and its links with large-scale modes of climate variability. *International Journal of Climatology*, *36*(14), 4439–4454. <https://doi.org/10.1002/joc.4642>
- Hevia-Cruz, F., Hildenbrand, A., & Sheldon, N. D. (2023). Climatic and landscape evolution of the Azores over the past million years: 2020–2023 geochemical and geochronological data (Version 1) [Dataset]. *Mendeley Data*. <https://doi.org/10.17632/fdzjhb26wz.1>
- Hevia-Cruz, F., Hildenbrand, A., Sheldon, N. D., Hren, M. T., Zanon, V., Marques, F. O., et al. (2024). Weathering pulses during glacial-interglacial transitions: Insights from well-dated paleosols in the Azores volcanic province (Central North Atlantic). *Quaternary Science Reviews*, *324*, 108438. <https://doi.org/10.1016/j.quascirev.2023.108438>
- Hildenbrand, A., Gillot, P., & Marlin, C. (2008). Geomorphological study of long-term erosion on a tropical volcanic ocean island: Tahiti-Nui (French Polynesia). *Geomorphology*, *93*(3–4), 460–481. <https://doi.org/10.1016/j.geomorph.2007.03.012>
- Hildenbrand, A., Madureira, P., Marques, F. O., Cruz, I., Henry, B., & Silva, P. (2008). Multi-stage evolution of a sub-aerial volcanic ridge over the last 1.3 Myr: S. Jorge Island, Azores Triple Junction. *Earth and Planetary Science Letters*, *273*(3–4), 289–298. <https://doi.org/10.1016/j.epsl.2008.06.041>

- Hildenbrand, A., Marques, F. O., & Catalão, J. (2018). Large-scale mass wasting on small volcanic islands revealed by the study of Flores Island (Azores). *Scientific Reports*, 8(1), 13898. <https://doi.org/10.1038/s41598-018-32253-0>
- Hildenbrand, A., Marques, F. O., Costa, A. C. G., Sibrant, A. L. R., Silva, P. F., Henry, B., et al. (2012). Reconstructing the architectural evolution of volcanic islands from combined K/Ar, morphologic, tectonic, and magnetic data: The Faial Island example (Azores). *Journal of Volcanology and Geothermal Research*, 241, 39–48. <https://doi.org/10.1016/j.jvolgeores.2012.06.019>
- Hildenbrand, A., Weis, D., Madureira, P., & Marques, F. O. (2014). Recent plate re-organization at the Azores Triple Junction: Evidence from combined geochemical and geochronological data on Faial, S. Jorge and Terceira volcanic islands. *Lithos*, 210, 27–39. <https://doi.org/10.1016/j.lithos.2014.09.009>
- Holdridge, L. R. (1947). Determination of world plant formations from simple climatic data. *Science*, 105(2727), 367–368. <https://doi.org/10.1126/science.105.2727.367>
- Hren, M. T., & Sheldon, N. D. (2012). Temporal variations in lake water temperature: Paleoenvironmental implications of lake carbonate  $\delta^{18}\text{O}$  and temperature records. *Earth and Planetary Science Letters*, 337, 77–84. <https://doi.org/10.1016/j.epsl.2012.05.019>
- Hurrell, J. W., & Van Loon, H. (1997). Decadal variations in climate associated with the North Atlantic Oscillation. *Climatic Change*, 36(3–4), 301–326. <https://doi.org/10.1023/A:1005314315270>
- Jenny, H. J. (1941). *Factors in soil formation*. McGraw-Hill.
- Kim, J. H., Meggers, H., Rimbau, N., Lohmann, G., Freudenthal, T., Müller, P. J., & Schneider, R. R. (2007). Impacts of the North Atlantic gyre circulation on Holocene climate off northwest Africa. *Geology*, 35(5), 387–390. <https://doi.org/10.1130/G23251A.1>
- Le Bas, M. J., Le Maitre, R. W., Streckeisen, A., & Zanettin, B., & IUGS Subcommittee on the Systematics of Igneous Rocks. (1986). A chemical classification of volcanic rocks based on the total alkali-silica diagram. *Journal of Petrology*, 27(3), 745–750. <https://doi.org/10.1093/ptrology/27.3.745>
- Lisiecki, L., & Raymo, M. (2005). A Pliocene-Pleistocene stack of 57 globally distributed benthic  $\delta^{18}\text{O}$  records. *Paleoceanography*, 20(1), PA1003. <https://doi.org/10.1029/2004PA001071>
- Louvat, P., & Allègre, C. J. (1998). Riverine erosion rates on Sao Miguel volcanic island, Azores archipelago. *Chemical Geology*, 148(3–4), 177–200. [https://doi.org/10.1016/S0009-2541\(98\)00028-X](https://doi.org/10.1016/S0009-2541(98)00028-X)
- Mack, G., James, W., & Monger, H. (1993). Classification of paleosols. *Geological Society of America Bulletin*, 105(2), 129–136. [https://doi.org/10.1130/0016-7606\(1993\)105%3C0129:COP%3E2.3.CO;2](https://doi.org/10.1130/0016-7606(1993)105%3C0129:COP%3E2.3.CO;2)
- Marbut, C. F. (1935). *Atlas of American agriculture. III. Soils of the United States*. Government Printing Office.
- Margari, V., Skinner, L. C., Tzedakis, P. C., Ganopolski, A., Vautravers, M., & Shackleton, N. J. (2010). The nature of millennial-scale climate variability during the past two glacial periods. *Nature Geoscience*, 3(2), 127–131. <https://doi.org/10.1038/ngeo740>
- Marques, F. O., Hildenbrand, A., & Hübscher, C. (2018). Evolution of a volcanic island on the shoulder of an oceanic rift and geodynamic implications: S. Jorge Island on the Terceira Rift, Azores Triple Junction. *Tectonophysics*, 738, 41–50. <https://doi.org/10.1016/j.tecto.2018.05.012>
- Martin-Garcia, G. M. (2019). Oceanic impact on European climate changes during the Quaternary. *Geosciences*, 9(3), 119. <https://doi.org/10.3390/geosciences9030119>
- Martrat, B., Grimalt, J. O., Shackleton, N. J., de Abreu, L., Hutterli, M. A., & Stocker, T. F. (2007). Four climate cycles of recurring deep and surface water destabilizations on the Iberian margin. *Science*, 317(5837), 502–507. <https://doi.org/10.1126/science.1139994>
- Maynard, J. (1992). Chemistry of modern soils as a guide to interpreting Precambrian paleosols. *The Journal of Geology*, 100(3), 279–289. <https://doi.org/10.1086/629632>
- Meirelles, M., Carvalho, F., Porteiro, J., Henriques, D., Navarro, P., & Vasconcelos, H. (2022). Climate change and impact on renewable energies in the Azores strategic visions for sustainability. *Sustainability*, 14(22), 15174. <https://doi.org/10.3390/su142215174>
- Melo, C. D., Maduro Dias, C. S., Wallon, S., Borba, A. E., Madruga, J., Borges, P. A., et al. (2022). Influence of climate variability and soil fertility on the forage quality and productivity in Azorean pastures. *Agriculture*, 12(3), 358. <https://doi.org/10.3390/agriculture12030358>
- Orr, T. J., Roberts, E. M., Wurster, C. M., Mtelega, C., Stevens, N. J., & O'connor, P. M. (2021). Paleoclimate and paleoenvironment reconstruction of paleosols spanning the Lower to Upper Cretaceous from the Rukwa Rift Basin, Tanzania. *Palaeogeography, Palaeoclimatology, Palaeoecology*, 577, 110539. <https://doi.org/10.1016/j.palaeo.2021.110539>
- Pinto, J. G., & Raible, C. C. (2012). Past and recent changes in the North Atlantic oscillation. *Wiley Interdisciplinary Reviews: Climate Change*, 3(1), 79–90. <https://doi.org/10.1002/wcc.150>
- Rad, S., Cerdan, O., Rivié, K., & Grandjean, G. (2011). Age of river basins in Guadeloupe impacting chemical weathering rates and land use. *Applied Geochemistry*, 26, S123–S126. <https://doi.org/10.1016/j.apgeochem.2011.03.046>
- Rad, S., Rivié, K., Vittecoq, B., Cerdan, O., & Allègre, C. J. (2013). Chemical weathering and erosion rates in the Lesser Antilles: An overview in Guadeloupe, Martinique and Dominica. *Journal of South American Earth Sciences*, 45, 331–344. <https://doi.org/10.1016/j.jsames.2013.03.004>
- Renne, P. R., Swisher, C. C., Deino, A. L., Karner, D. B., Owens, T. L., & DePaolo, D. J. (1998). Intercalibration of standards, absolute ages and uncertainties in  $^{40}\text{Ar}/^{39}\text{Ar}$  dating. *Chemical Geology*, 145(1–2), 117–152. [https://doi.org/10.1016/S0009-2541\(97\)00159-9](https://doi.org/10.1016/S0009-2541(97)00159-9)
- Retallack, G. (2001). *Soils of the past: An introduction to paleopedology* (2nd ed.). Blackwell Science.
- Rodrigues, T., Alonso-García, M., Hodell, D. A., Rufino, M., Naughton, F., Grimalt, J. O., et al. (2017). A 1-Ma record of sea surface temperature and extreme cooling events in the North Atlantic: A perspective from the Iberian Margin. *Quaternary Science Reviews*, 172, 118–130. <https://doi.org/10.1016/j.quascirev.2017.07.004>
- Sánchez-Goni, M. F., Landais, A., Fletcher, W. J., Naughton, F., Desprat, S., & Duprat, J. (2008). Contrasting impacts of Dansgaard-Oeschger events over a western European latitudinal transect modulated by orbital parameters. *Quaternary Science Reviews*, 27(11–12), 1136–1151. <https://doi.org/10.1016/j.quascirev.2008.03.003>
- Santos, F. D., Valente, M. A., Miranda, P. M. A., Aguiar, A., Azevedo, E. B., Tomé, A. R., & Coelho, F. (2004). Climate change scenarios in the Azores and Madeira Islands. *World Resource Review*, 16(4), 473–491.
- Schwarz, W. H., & Trieloff, M. (2007). Intercalibration of  $^{40}\text{Ar}$ - $^{39}\text{Ar}$  age standards NL-25, HB3gr hornblende, GA1550, SB-3, HD-B1 biotite and BMus/2 muscovite. *Chemical Geology*, 242(1–2), 218–231. <https://doi.org/10.1016/j.chemgeo.2007.03.016>
- Sheldon, N. D. (2003). Pedogenesis and geochemical alteration of the Picture Gorge Subgroup, Columbia River basalt, Oregon. *GSA Bulletin*, 115(11), 1377–1387. <https://doi.org/10.1130/B25223.1>
- Sheldon, N. D. (2006). Quaternary glacial-interglacial climate cycles in Hawaii. *The Journal of Geology*, 114(3), 367–376. <https://doi.org/10.1086/500993>
- Sheldon, N. D., Retallack, G., & Tanaka, S. (2002). Geochemical climofunctions from North American soils and application to paleosols across the Eocene-Oligocene boundary in Oregon. *The Journal of Geology*, 110(6), 687–696. <https://doi.org/10.1086/342865>
- Sheldon, N. D., & Tabor, N. (2009). Quantitative paleoenvironmental and paleoclimatic reconstruction using paleosols. *Earth-Science Reviews*, 95(1–2), 1–52. <https://doi.org/10.1016/j.earscirev.2009.03.004>

- Sibrant, A., Hildenbrand, A., Marques, F., Weiss, B., Boulesteix, T., Hübscher, C., et al. (2015). Morpho-structural evolution of a volcanic island developed inside an active oceanic rift: S. Miguel Island (Terceira Rift, Azores). *Journal of Volcanology and Geothermal Research*, *301*, 90–106. <https://doi.org/10.1016/j.jvolgeores.2015.04.011>
- Soil Survey Staff. (2014). *Keys to soil taxonomy* (12th ed.). USDA-Natural Resources Conservation Service.
- Sowards, K. F., Nelson, S. T., McBride, J. H., Bickmore, B. R., Heizler, M. T., Tingey, D. D., et al. (2018). A conceptual model for the rapid weathering of tropical ocean islands: A synthesis of geochemistry and geophysics, Kohala Peninsula, Hawaii, USA. *Geosphere*, *14*(3), 1324–1342. <https://doi.org/10.1130/GES01642.1>
- Steiger, R. H., & Jäger, E. (1977). Subcommittee on geochronology: Convention on the use of decay constants in geo- and cosmochronology. *Earth and Planetary Science Letters*, *36*(3), 359–362. [https://doi.org/10.1016/0012-821X\(77\)90060-7](https://doi.org/10.1016/0012-821X(77)90060-7)
- Tabor, N. J., & Myers, T. S. (2015). Paleosols as indicators of paleoenvironment and paleoclimate. *Annual Review of Earth and Planetary Sciences*, *43*(1), 333–361. <https://doi.org/10.1146/annurev-earth-060614-105355>
- Taylor, S. H., Ripley, B. S., Woodward, F. I., & Osborne, C. P. (2011). Drought limitation of photosynthesis differs between C3 and C4 grass species in a comparative experiment. *Plant, Cell and Environment*, *34*(1), 65–75. <https://doi.org/10.1111/j.1365-3040.2010.02226.x>
- Thatcher, D. L., Wanamaker, A. D., Denniston, R. F., Asmerom, Y., Polyak, V. J., Fullick, D., et al. (2020). Hydroclimate variability from western Iberia (Portugal) during the Holocene: Insights from a composite stalagmite isotope record. *The Holocene*, *30*(7), 966–981. <https://doi.org/10.1177/0959683620908648>
- Tipple, B. J., & Pagani, M. (2007). The early origins of terrestrial C4 photosynthesis. *Annual Reviews of Earth and Planetary Science Letters*, *35*(1), 435–461. <https://doi.org/10.1146/annurev-earth.35.031306.140150>
- Wanner, H., Brönnimann, S., Casty, C., Gyalistras, D., Luterbacher, J., Schmutz, C., et al. (2001). North Atlantic Oscillation—concepts and studies. *Surveys in Geophysics*, *22*(4), 321–381. <https://doi.org/10.1023/A:1014217317898>
- West, A. J., Galy, A., & Bickle, M. (2005). Tectonic and climatic controls on silicate weathering. *Earth and Planetary Science Letters*, *235*(1–2), 211–228. <https://doi.org/10.1016/j.epsl.2005.03.020>
- White, R. E. (2005). *Principles and practice of soil science: The soil as a natural resource*. John Wiley & Sons.
- Wilson, S. A. (1997). The collection, preparation and testing of USGS reference material BCR-2, Columbia River Basalt. *US Geological Survey Open-File Report*.